The Leucine Zippers of the HLH-LZ Proteins Max and c-Myc Preferentially Form Heterodimers

C. Muhle-Goll,* M. Nilges, and A. Pastore

EMBL, Meyerhofstrasse 1, D-69117 Heidelberg, Germany

Received February 7, 1995; Revised Manuscript Received July 31, 1995[⊗]

ABSTRACT: c-Myc and Max are members of a subfamily of the helix−loop−helix transcription-regulating proteins. Their function is mediated by switches in the dimerization partners; c-Myc does not homodimerize *in vivo* but competes with Mad, another member of the subfamily, to form heterodimers with Max, leading to either activation or repression of transcription. Max is also able to form homodimers. In an attempt to identify which regions of the proteins carry the information to determine specific recognition of the dimerization partner, we have investigated the dimerization properties of synthetic peptides corresponding to the leucine zipper sequence of Max and c-Myc using circular dichroism and nuclear magnetic resonance techniques. We show that the heterodimer is obtained readily by simply mixing the peptides and that at neutral pH it is more stable than the homodimer of the Max leucine zipper. We have shown in a previous paper [Muhle-Goll, C. et al. (1994) *Biochemistry 33*, 11296-11306] that the leucine zipper of c-Myc does not form stable homodimers under these conditions. Thus, the leucine zipper regions of these two proteins by themselves display the same behavior as the entire proteins. However, even the heterodimer is less stable than dimers of leucine zippers of the basic leucine zipper family such as GCN4 and Fos-Jun. The specificity of the interaction between different monomers can be explained by polar interactions. We investigate the structural role of the polar and charged residues in the hydrophobic interface by molecular-modeling studies.

Two dimerization motifs are combined in the eukaryotic family of DNA-binding HLH-LZ[1] proteins: a helix−loop−helix (HLH) and a leucine zipper (LZ) domain. The former consists of two α-helices connected by a loop, C-terminally contiguous to a region rich in basic residues. The latter is characterized by a dimeric coiled coil structure with heptad repeats of leucines. Each of the motifs, HLH and LZ, is also present in other classes of transcriptional activators. Dimerization of the HLH-LZ proteins is required for binding of their specific DNA sequences. Formation of both homo- and heterodimers with other proteins of the family is possible in analogy with what is known to occur in the b-Zip family (Bohmann et al., 1987; Hai et al., 1989; Cao et al., 1991; Williams et al., 1991). It is now established that the molecular determinants for both DNA and partner specificity reside in the HLH-LZ region (Davis et al., 1990; Gregor et al., 1990; Hu et al., 1990a; Voronova & Baltimore, 1990; Beckmann & Kadesh, 1991; Fisher et al., 1991; Amati et al., 1993).

However, while the HLH and the LZ motifs are sufficient by themselves for mediation of dimerization in the HLH and b-Zip protein families, respectively, the role of the LZ domain in the HLH-LZ family is still less clear. Biological evidence suggests that it plays a role in the specificity of the interaction between monomers. This has been shown for the dimerization partners c-Myc and Max, both members of the HLH-LZ family; deletion of either the HLH or the LZ (Kato et al., 1992; Davis & Halazonetis, 1993) or swapping of the LZ with the analogous region of Fos eliminates the ability of c-Myc to bind to Max. Swapping the HLH region with the corresponding region of TFEB, another HLH-LZ protein, generates a mutant still able to interact with Max (Davis & Halazonetis, 1993).

Recently, extensive investigations have been carried out to determine the rules that govern the choice of dimerization partners in proteins containing coiled coils. Members of the b-Zip family [for review, see Baxevanis and Vinson (1993)] and model peptides derived from tropomyosin (Zhou et al., 1994, and references cited therein) have been used to show that the stability of a dimer is predominantly governed by polar interactions between amino acids on e and g positions and hydrophobic interactions between amino acids on a and d positions (Krylov et al., 1994). To assess if the same positions in the LZ of HLH-LZ proteins are important for dimerization, Amati and colleagues generated complementary mutants by reciprocally exchanging e and g positions in the LZ of c-Myc and Max (Amati et al., 1993). The mutants were able to bind to species in which complementary exchanges had been performed.

We have chosen a different approach to address questions about the contribution of the LZ to stability and specificity of monomer−monomer interactions in HLH-LZ proteins. We have studied the structural properties of isolated HLH-LZ leucine zippers and analyzed their properties in the formation of both homo- and heterodimers. In a previous report, we have shown by CD and NMR experiments that the LZ regions of different HLH-LZ proteins can have drastically

* To whom correspondence should be addressed.

[⊗] Abstract published in *Advance ACS Abstracts,* October 1, 1995.

[1] Abbreviations: HLH, helix−loop−helix; LZ, leucine zipper; b-Zip, basic leucine zipper; Max-LZ and Myc-LZ, synthetic peptides spanning the sequence of the leucine zipper region of Max and Myc, respectively; CD, circular dichroism; NMR, nuclear magnetic resonance; ppm, parts per million; TPPI, time-proportional phase incrementation; TOCSY, total correlation spectroscopy; NOE, nuclear Overhauser enhancement; NOESY, 2D NOE spectroscopy; TFE, trifluoroethanol; T_m, melting temperature.

0006-2960/95/0434-13554$09.00/0

different abilities to form homodimers (Muhle-Goll et al., 1994). While the LZ of TFEB can form a homodimer at neutral pH, homodimers of the LZ of c-Myc could only be detected at acidic pH in the presence of divalent anions, indicating that electrostatic repulsion prevents the formation of homodimers at neutral pH. Even under most favorable conditions, both LZs showed only a moderate stability when compared to peptides derived from LZ of the b-Zip family (GCN4, Weiss, 1990; Thompson et al., 1993; Fos/Jun, O'Shea et al., 1992).

The question which we address in this paper is whether isolated LZs are still able to preferentially form heterodimers and how stable this interaction is. This should ultimately shed light on the mechanism which determines the transcription regulation. An obvious choice for this study is the interaction between c-Myc, which we have already characterized, and Max. Among the proteins closely related to Myc, Max plays a central role [for review, see Evan and Littlewood (1993)]. It is the only protein of the subfamily able to form stable homodimers under physiological conditions (Blackwood & Eisenman, 1991; Ayer et al., 1993; Zervos et al., 1993). The structure of the HLH-LZ region has been solved, showing a stable dimerization interface to which both subdomains contribute (Ferré-D'Amaré et al., 1993). c-Myc, Mad, and Mxi1 do not homodimerize but compete with each other in heterodimer formation with Max (Ayer & Eisenman, 1993; Larsson et al., 1994). Max is constitutively expressed, highly stable, and more abundant than c-Myc or Mad. In contrast to Max, both c-Myc and Mad have short half-lives (Ayer & Eisenman, 1993) and their expression is regulated. Complexed to Max, c-Myc exerts its function as a specific DNA-binding transcriptional activator. Mad represses transcription when bound to Max and thus acts as an antagonist of c-Myc. We characterize the Max-LZ homodimer and the heterodimer between c-Myc-LZ and Max-LZ by CD and NMR studies and support the interpretation of the results by molecular-modeling studies.

MATERIALS AND METHODS

Amino Acid Sequences. Sequences were extracted from the SwissProt database (Bairoch & Boeckmann, 1991). The LZ boundaries were chosen taking the X-ray structure of the HLH-LZ domain of Max as a reference (Ferré-D'Amaré et al., 1993). The sequences extend from one residue before the first residue of the LZ region to three residues after the last conserved leucine. The peptides have the following sequences (the d positions are numbered): Max-LZ, NH_2-YM^{2}RRKNHTH^{9}QQDIDDL^{16}KRQNALL^{23}EQQVRAL^{30}-EKA-COOH; and Myc-LZ, NH_2-SV^{2}QAEEQKL^{9}ISEEDLL^{16}-RKRREQL^{23}KHKLEQL^{30}RNS-COOH.

Peptide Synthesis. The peptides were synthesized and purified by the EMBL Peptide Synthesis Group using standard solid phase methods as described (Frank & Gausepohl, 1988). Peptide purity (≥98%) was determined by HPLC, and composition was confirmed by electrospray mass spectrometry.

Circular Dichroism Spectroscopy. Circular dichroism measurements were carried out on a Jasco J710 instrument equipped with a Neslab (model RTE-100) water bath. The spectrometer was calibrated using the ammonium salt of 10-(+)-camphorsulfonic acid. Quartz cells of various path lengths were used. Spectra were obtained on samples containing between 10 and 1000 μM peptide at various pH values and salt concentrations. Spectra under acidic conditions and at neutral pH were measured in 20 mM formate buffer (pH 3.0) and 20 mM Tris-HCl buffer (pH 7.5), respectively, unless otherwise specified. The spectra shown are averaged over 5−10 scans and normalized for concentration and path length to obtain the mean residue ellipticity after subtraction of the buffer contribution. Temperature scans were performed by scanning continuously at a constant wavelength of 222 nm from 3 to 86 °C with 0.2 °C steps at a scan rate of 10 °C/h using the Time Scan Mode of Jasco J710 and were completely reversible. The degree of α-helicity was determined from the intensity of the ellipticity at 222 nm, assuming a value of $-33\,400°$ cm^{-2} dmol^{-1} for a 100% α-helical peptide of comparable length (Chen et al., 1974). The molar fraction of unfolded peptide, U, was calculated as $U = (\Theta_{222} - \Theta_N)/(\Theta_U - \Theta_N)$, where Θ_N is the ellipticity of the native species and Θ_U that of the denatured one, as calculated by a least squares fit of the base lines preceding and following the transition region.

Titrations of Max-LZ with Myc-LZ were performed at pH 7.5 (20 mM Tris-HCl and 20 mM NaF), 17 °C, so that the total peptide concentration was kept constant. Different total peptide concentrations between 20 μM and 1 mM were used. The spectra were processed with the program SNARF (van Hoesel, University of Groningen, 1992) and plotted with GNUPLOT.

Nuclear Magnetic Resonance Measurements. The NMR measurements were performed on a 500 MHz Bruker AMX spectrometer. They were carried out using 2−4 mM samples in 90% H_2O/10% D_2O solutions at pH 5.6 and 6.9. 2D spectra were acquired at 27 and 17 °C to resolve possible overlap. Samples of equimolar amounts of Myc-LZ and Max-LZ were prepared by mixing the corresponding amounts of stock solution of the two peptides at pH 5.6 and leaving them overnight at room temperature. 2D spectra were recorded in phase-sensitive mode (Marion & Wüthrich, 1983) with water proton-frequency irradiation. Clean-TOCSY spectra (Griesinger et al., 1988) were measured using the TOWNY composite pulse cycle (Kadkhodaei et al., 1993). Mixing times used were 200 ms (Max-LZ and Max-LZ/Myc-LZ) and 300 ms (Myc-LZ) in the NOESY experiments (Jeener et al., 1979; Macura et al., 1981) and 45−60 ms for the TOCSY experiments. Data were processed on a Bruker X32 station using the UXNMR program. The AURELIA program was used for displaying and plotting spectra.

Model Building. 3D models of the dimers were calculated using the program X-PLOR (Brünger, 1992) on the basis of the X-ray crystal structure of the GCN4 LZ (O'Shea et al., 1991). The side chains of c-Myc and Max were built onto the backbone of GCN4 as described (Nilges & Brünger, 1991). The resulting structures were energy-minimized using molecular dynamics and conjugate gradient minimization. Force field, molecular dynamics protocol, solvent corrections, and restraints for backbone hydrogen bonds and the distance between the monomers were also used as described (Nilges & Brünger, 1991). In addition, a potential for the charged side chains (Glu, Asp, Lys, and Arg) was introduced to prevent close contacts of like charges and favor salt bridges using ambiguous distance restraints (Nilges, 1995). One attractive restraint was added from each charged side chain to all other side chains with opposite charge. This restraint is satisfied if any of these is closer than 6 Å. In a similar way, one repulsive restraint was added from each charged side chain to all other side chains of like charge. This

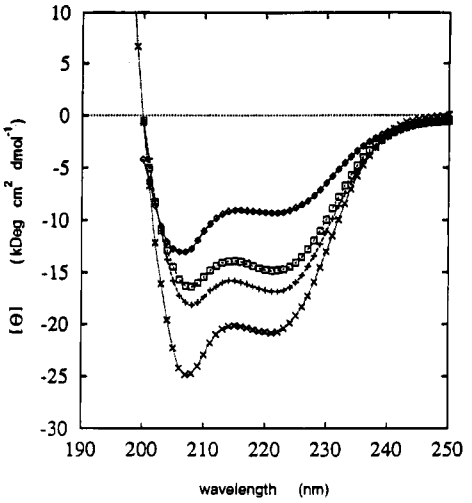

FIGURE 1: Effect of pH and salt on the circular dichroism spectra of Max-LZ, 1 mM, at 18 °C. The symbols represent the following conditions: (◇) pH 3.0, no salt; (+) pH 3.0, 50 mM Na_2SO_4; (□) pH 7.5, 20 mM NaF; and (×) 20 mM NaF/TFE (1:1).

restraint is satisfied if none of them is closer than 5 Å. This restraining potential improved the number of correctly predicted salt bridges in test calculations with GCN4 (M. Nilges, unpublished results). No refinement in explicit solvent was performed.

RESULTS

CD Measurements: Probing Heterodimer Formation

(A) Max-LZ. Typical CD spectra of Max-LZ are shown in Figure 1. The two minima around 208 and 222 nm are characteristic features of α-helical structure. Various salt and pH conditions were screened (part a of Table 1). In the presence of salt, Max-LZ is sensitive to pH conditions only to a minor extent. The maximal percentage of helicity for a 1 mM peptide solution was around 50−51% (Table 1). In 50% TFE, a helix-stabilizing solvent, the helicity reaches a value of 62%.

The thermal denaturation of Max-LZ was studied at acidic pH in the presence of 50 mM Na_2SO_4 (Figure 2A) and at neutral pH (Tris-HCL buffer) in the presence of 20 mM NaF (Figure 2B). These were the salt conditions under which Myc homodimers had been found most helical at the two pHs (Muhle-Goll et al., 1994). Under both conditions, Max-LZ shows a cooperative transition as can be derived from the sigmoidic shape of the curves which implies a two-state transition. The melting temperature, defined as the temperature where 50% of the peptide is in the unfolded state, increases with the peptide concentration as is shown in Figure 2A,B.

The concentration dependence of the T_m values of Max-LZ can be analyzed assuming a monomer-to-dimer equilibrium. Starting with folded dimers (F_2), the transition leads to unfolded monomers (U) via folded monomers (F) as intermediates. The unfolding reaction can be described by

$$F_2 \overset{K_1}{\rightleftharpoons} 2F \overset{K_2}{\rightleftharpoons} 2U$$

where

$$K_1 = [F]^2/[F_2] \quad \text{and} \quad K_2 = [U]/[F]$$

If we assume that the folded monomer is not present at significant concentrations in the equilibrium, as expected for an amphiphilic helical peptide of this size, the unfolding reaction can be simplified as

$$F_2 \overset{K_u}{\rightleftharpoons} 2U$$

where

$$K_u = [U]^2/[F_2] = 2P_t[f_U^2/(1 - f_U^2)]$$

P_t is the total peptide concentration and f_U the molar fraction of unfolded peptide as judged from the ellipticity at 222 nm. From these equations, K_u, the dimer dissociation constant, was calculated from the intensities of the ellipticity at 222 nm in the transition zone at each different temperature and concentration. Similar analysis can be done by assuming different two-state stoichiometries. If we report the values of K_u calculated for different concentrations in a van't Hoff plot, we may check the assumption made that the two-step equilibrium involves a monomer-to-dimer transition rather than a monomer-to-higher species one. Only for a monomer-to-dimer equilibrium can the data be fitted by the same straight line within the experimental error as expected for this stoichiometry (Figure 2C,D). The K_u obtained at 298 °C is 20.3 × 10^{-5} M^{-1} at pH 7.5 (±5%) and 8.5 × 10^{-5} M^{-1} at pH 3.0 (±8%).

(B) Myc-LZ. Most of the work on Myc-LZ has been discussed extensively before (Muhle-Goll et al., 1994) and is summarized here only briefly. Myc-LZ was shown to be only about 50% α-helical at pH 7 compared to 76% at pH 3 in the presence of sulfate (T = 4 °C). The maximal

Table 1: Percentage of α-Helical Secondary Structure Determined by CD Measurements at 18 °C under Various pH and Salt Conditions of (a) Max-LZ and (b) Max-LZ/Myc-LZ[a]

pH	medium	helical content (%)
	(a) Max-LZ	
	water	
3.0	no salt	28
4.8	no salt	46
5.5	no salt	43
6.9	no salt	48
7.5	no salt	51
8.2	no salt	45
	20 mM formate	
3.0	no salt	28
3.0	20 mM NaF	47
3.0	20 mM Na_2SO_4	51
3.0	20 mM $MgSO_4$	49
3.0	20 mM Na_2HPO_4	45
	20 mM Tris-HCL	
7.5	no salt	51
7.5	20 mM NaF	47
7.5	20 mM Na_2SO_4	46
7.5	20 mM $MgSO_4$	47
7.5	20 mM Na_2HPO_4	49
3.0	50% TFE, 50 mM Na_2SO_4	62
	(b) Max-LZ/Myc-LZ	
3.6	water	34
4.9	water, 100 mM NaF	56
5.6	10 mM sodium acetate	54
	20 mM Tris-HCL	
6.1	no salt	55
7.5	no salt	53
7.5	20 mM NaF	54
7.5	100 mM NaF	56
7.5	50 mM Na_2SO_4	55

[a] The peptide concentrations were 1 mM.

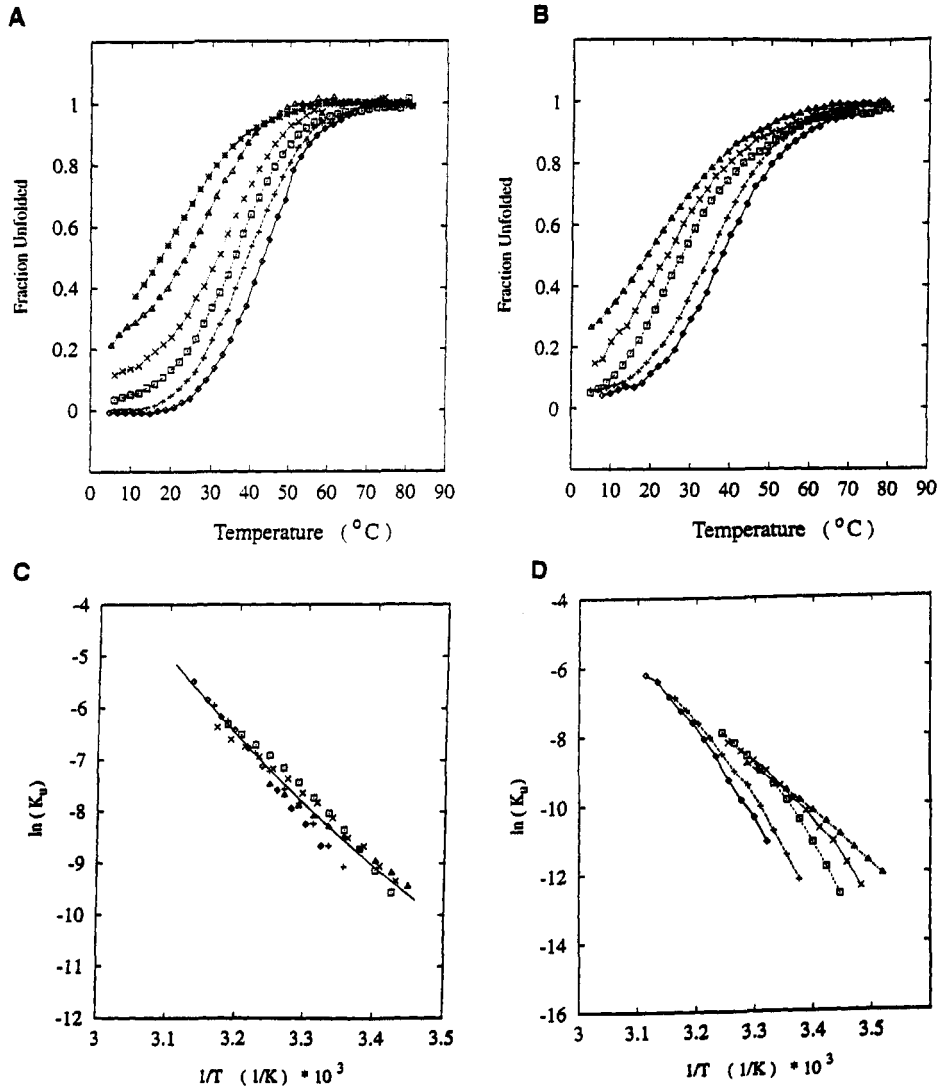

FIGURE 2: (A) Concentration dependence of the thermal denaturation of Max-LZ at pH 3.0, 50 mM Na_2SO_4. Temperature dependence of the mean residue ellipticity (Θ) at 222 nm plotted as fraction of unfolded peptide. Peptide concentrations were 910 (◇), 700 (+), 350 (□), 200 (×), 100 (△), and 20 μM (*). (B) Same as part A, but at pH 7.5, 20 mM NaF. Peptide concentrations were 1100 (◇), 700 (+), 350 (□), 200 (×), and 100 μM (△). (C and D) van't Hoff plots of the thermal denaturation of Max-LZ at pH 7.5. Conditions and symbols used were as in part B. The equilibrium constants were calculated as described in the Results assuming a dimer-to-monomer and a tetramer-to-monomer equation (C and D, respectively). The solid line in part C is a least-squares fit of the experimental data. Lines in part D link data points corresponding to the same concentration. The figures clearly indicate that the best fitting of the data is produced by assuming the presence of a dimer-to-monomer equilibrium.

ellipticity (82%) was obtained in 50% TFE/aqueous solution. In thermal denaturation studies, we were able to measure a cooperative transition at acidic pH, with T_m values dependent on the concentration. In contrast, no concentration dependence could be detected at pH 7 in the temperature range studied. Thus, at neutral pH, the monomer-to-homodimer equilibrium of Myc-LZ seems to be strongly shifted in favor of the monomer. If the ellipticity value at 222 nm obtained at acidic pH and low temperatures is chosen as a reference for the fully folded dimeric species, the thermal denaturation curves show that more than 50% of Myc-LZ at neutral pH is already in an unfolded state even at low temperatures.

(C) Max-LZ/Myc-LZ. Since no pH dependence in the range of 4.9 to 8.0 could be detected, the Max-LZ/Myc-LZ mixture was studied only at physiological pH. Various buffer conditions were screened by CD for stabilization of the helical signal (see part b of Table 1). To ascertain that equilibrium was reached when the peptides were mixed, samples containing equimolar amounts of Max-LZ and Myc-LZ were first heated above the melting temperature and successively cooled slowly. The values of the ellipticity before and after did not differ from each other. Immediate formation of a heterospecies upon mixing can be therefore assumed. An increase of the CD signal of approximately 30% and 20% from the values of Max-LZ and Myc-LZ, respectively, takes place upon mixing (Figure 3). A similar effect is demonstrated by the thermal denaturation behavior (Figure 4A). Higher temperatures are required (approximately 7 °C) to break the heterospecies into monomers (Figure 4A,B), though the melting temperatures remain concentration dependent within approximately the same range as measured for Max-LZ.

Stoichiometry of the Complex. Titration of Max-LZ with Myc-LZ at various total peptide concentrations in the range of 20 μM to 1 mM was performed to ascertain that the increase of the ellipticity upon mixing is not due to nonspecific aggregation of the two peptides. The total peptide concentration during a titration experiment was kept constant. The observed stabilization of the helical signal did not depend on the total peptide concentration (data not shown). Figure

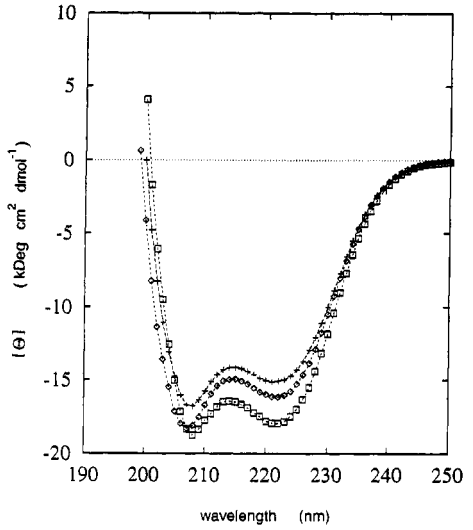

FIGURE 3: Comparison of CD spectra of Max-LZ and Myc-LZ with an equimolar mixture of the two peptides. The spectra were recorded at 18 °C, pH 7.5, 20 mM NaF, and 1 mM peptide concentration. The symbols represent the following conditions: (+) Max-LZ, (◇) Myc-LZ, and (□) Max-LZ/Myc-LZ.

5 shows the dependence of the ellipticity at 222 nm on the ratio Max-LZ/entire peptide concentration. The best fit polynomial curve has a minimum at a ratio of Max-LZ/entire peptide concentration of 0.5. This suggests a 1:1 complex formation of a heterospecies. An analysis similar to that described above for Max-LZ shows also that the data for the Max-LZ/Myc-LZ are only compatible with a dimer-to-monomer equilibrium with a K_u of 6.13×10^{-5} $M^{-1} \pm 9\%$ (calculated at neutral pH and 25 °C) (Figure 6A,B).

NMR Measurements: A More Detailed Analysis of the Secondary Structure

Myc-LZ and Max-LZ Homodimers. The 2D NMR spectra of separate solutions of Myc-LZ and Max-LZ at pH 5.6 were assigned by using conventional sequential assignment techniques (Wüthrich, 1986). The pH was chosen as a compromise between the conditions used for CD studies and the one optimal for observing amide connectivities. Spin system assignments were initially obtained from 2D TOCSY experiments at 290 °C. 2D NOESY spectra were 200 ms (Max-LZ) and 300 ms (Myc-LZ) mixing times were used to identify short range NOEs between HN−HN(i,i+1), Hα−HN(i,i+1), Hβ−HN(i,i+1), and Hα−Hβ(i,i+3) connecting the previously identified spin systems. To help the assignment of Max-LZ, additional TOCSY and NOESY 2D NMR experiments were performed at pH 6.9 and 40 mM NaCl, conditions under which CD measurements had shown a slightly higher α-helical content for this peptide.

Max-LZ/Myc-LZ Heterodimers. A similar procedure was applied to the spectrum assignment of an equimolar ratio of Myc-LZ and Max-LZ at pH 5.6 and 27 °C. Comparison of the TOCSY spectrum with the ones of the single peptides aided the assignment of several spin systems. Comparison with spectra measured at 17 °C confirmed the assignment. The proton chemical shifts of both Max-LZ and Myc-LZ homo- and heterodimers are given in parts a and b of Table 2, respectively. The HN−HN regions of the NOESY spectra of Max-LZ, Myc-LZ, and the mixture of the two peptides are compared in Figure 7A−C. All three parts of Figure 7 show HN−HN(i,i+1) NOE cross-peaks typical of α-helical secondary structure. The absolute number of cross-peaks

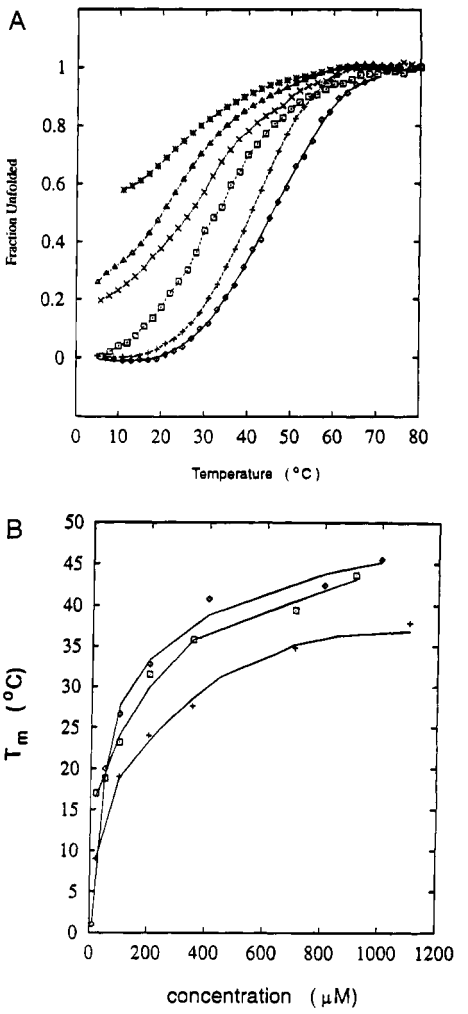

FIGURE 4: (A) Temperature dependence of the mean residue ellipticity (Θ) at 222 nm of an equimolar mixture of Max-LZ and Myc-LZ, pH 7.5, 20 mM NaF, plotted as fraction unfolded. Peptide concentrations were 1000 (◇), 400 (+), 200 (□), 100 (×), 50 (△), and 10 μM (*). (B) Comparison of the concentration dependence of the melting temperatures, T_m, of Max-LZ, pH 3.0, 50 mM Na_2SO_4 (□), and Max-LZ, pH 7.5, 20 mM NaF (+), with the equimolar mixture of Max-LZ and Myc-LZ, pH 7.5, 20 mM NaF (◇). Solid lines are computer-generated curves, obtained by a polynomial fit of the experimental data.

increases if the peptides are mixed. Since the chemical shift dispersion also increases, this effect cannot be simply explained as an additive effect of the HN−HN NOEs already present in the spectra of the separated Max-LZ and Myc-LZ but must indicate a change of the conformation occurring upon heterodimer formation.

Hα Frequency Shifts. The difference between the Hα frequencies of the peptides in the mixture and in separate solutions is shown for each residue in Figure 8. For Max-LZ (Figure 8A) and to a smaller amount for Myc-LZ (Figure 8B), a general upfield shift of the Hα resonances can be observed. An upfield shift throughout the sequence with respect to the random coil values is characteristic of helical structure (Pastore & Saudek, 1990; Wishart et al., 1991). The upfield shift of the Hα resonances upon mixing the peptides can thus be interpreted as a stabilization of the α-helical secondary structure.

Model Building

The models served to visualize the conformations of the side chains in different dimers and allow a qualitative interpretation of the results of NMR and CD beyond what

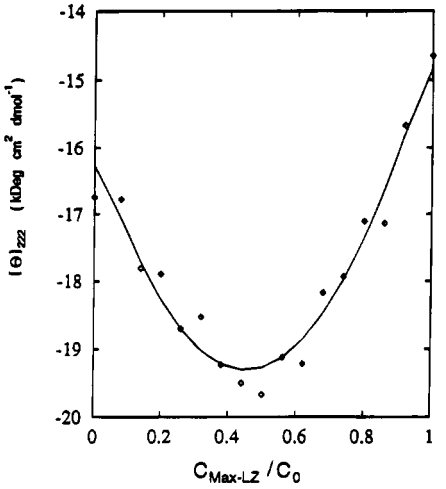

FIGURE 5: Dependence of the mean residue ellipticity (Θ) at 222 nm on the ratio of the two peptides in the mixture. Conditions were pH 6.9, 5 mM BTP, 20 mM NaF, and 17 °C. The entire peptide concentration (C_0) was kept constant at 1 mM, and the concentration of Max-LZ (C_{Max-LZ}) and Myc-LZ varied accordingly.

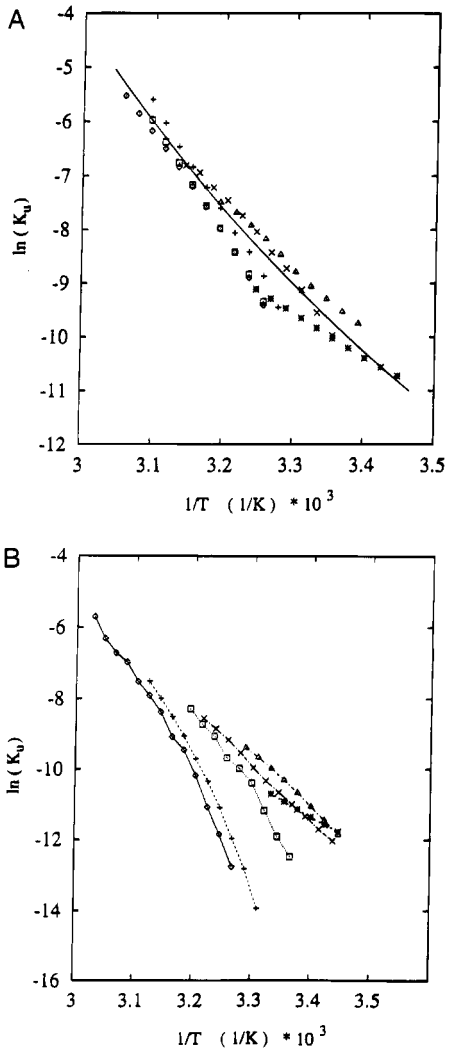

FIGURE 6: (A and B) van't Hoff plots of the thermal denaturation of an equimolar mixture of Max-LZ and Myc-LZ (pH 7.5, 20 mM NaF). Conditions and symbols used were as in Figure 4A. The equilibrium constants were calculated assuming a dimer-to-monomer and a tetramer-to-monomer equation (A and B, respectively).

is possible from the helical wheel representations (Figure 9). A representative model of a Max-LZ/Myc-LZ heterodimer is shown in Figure 10. Figure 10A shows the interactions around Glu12 in Myc-LZ, interactions of Asn20 of Max-LZ with the main chain of Myc-LZ, and a polar interaction between Arg20 of Myc-LZ and Asn20 of Max-LZ. Figure 10B shows two of the three salt bridges between the two monomers that have formed in the models, between Max-LZ-Glu31 and Myc-LZ-Lys26, and Max-LZ-Glu24 and Myc-LZ-Arg19.

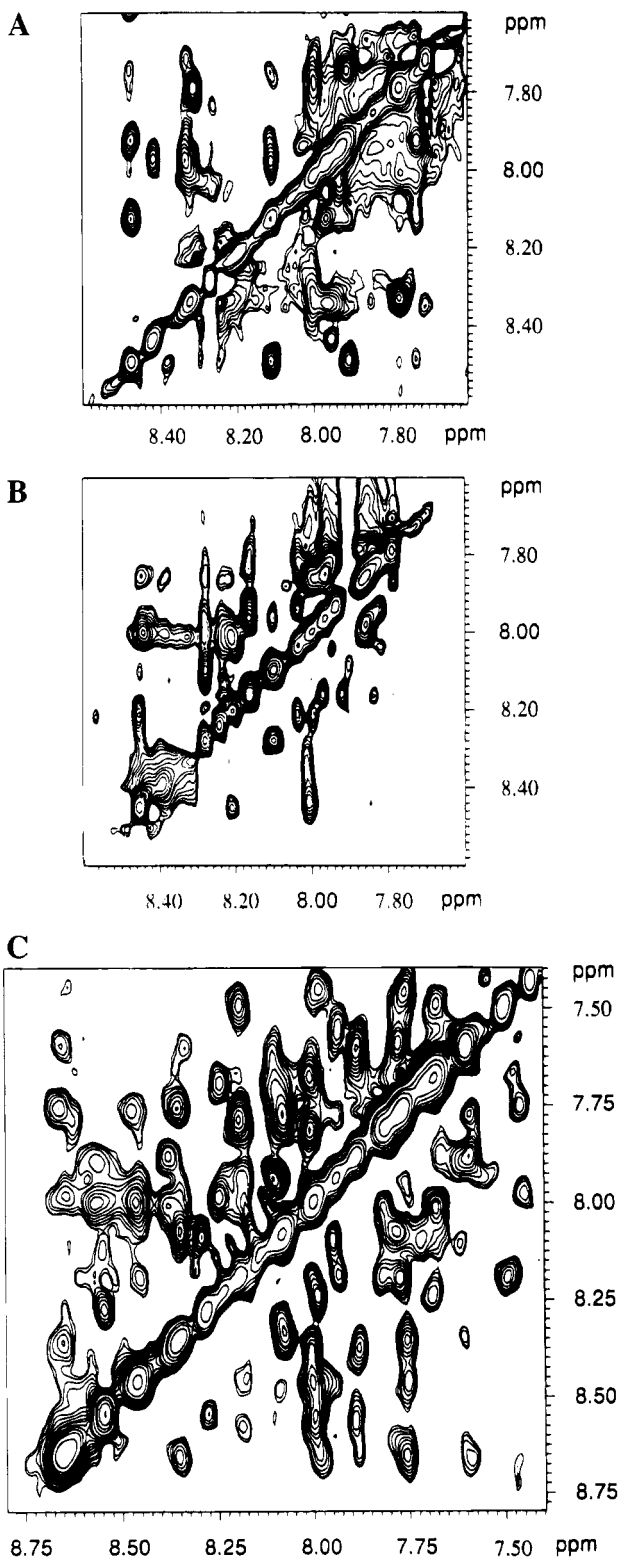

FIGURE 7: Comparison of the NH−NH regions of the NOESY spectra of the peptides at pH 5.6 and 290 K. Mixing times were 200 ms for Max-LZ and Max-LZ/Myc-LZ and 300 ms for Myc-LZ: (A) Max-LZ, 2.9 mM; (B) Myc-LZ, 4.0 mM; and (C) Max-LZ/Myc-LZ, 2.9 mM.

Table 2: Proton Chemical Shifts of (a) Max-LZ and (b) Myc-LZ[a]

residue	chemical shifts (ppm)					
	HN	Hα	Hβ	Hγ	Hδ	Hε/others
			(a) Max-LZ			
Tyr1		3.834	2.964		6.983	6.715
		3.994	2.895		6.890	6.644
Met2	8.457	4.326	1.803	2.368		
	8.134	4.242	1.779	2.282		
Arg3	8.422	4.154	1.694, 1.588	1.519	3.075	7.130
	8.310	4.064	1.601, 1.545	1.440	2.996	7.066
Arg4	8.443	4.204	1.705	1.604, 1.492	3.048	7.130
	8.340	4.136	1.614	1.524, 1.433	2.992	
Lys5	8.430	4.134	1.636	1.295	1.529	2.887
	8.369	4.073	1.701	1.244	1.495	2.798
Asn6			3.054, 2.993			
	8.428	4.462	2.620			
His7	8.413	4.435	3.053, 3.131		8.272	7.095
	8.236	4.462	2.954, 3.025			6.997
Thr8	8.187	4.366		1.078		
	8.106	4.335	4.277	1.022		
His9	8.736	4.447	3.078		7.064	8.231
	8.630	4.458	3.038			
Gln10	8.421	3.846	1.989, 1.835	2.248		7.721, 6.803
	8.612	3.707	2.085, 1.893	2.299		7.615, 6.782
Gln11	7.958	4.020	1.982	2.271		7.602, 6.769
	7.999	3.928	2.026	2.218		7.497, 6.679
Asp12	7.977	4.426	2.783, 2.595			
	7.674	4.317	2.753, 2.465			
Ile13	7.966	3.585	1.844	1.328, 0.777	0.636	
	8.074	3.415	1.822	0.806	0.676	
Asp14	8.338	4.273	2.631, 2.592			
	8.348	4.167	2.595, 2.486			
Asp15	8.317	4.376	2.760, 2.612			
	8.080	4.328	2.737, 2.604			
Leu16	7.780	3.965	1.620	1.295	0.801, 0.716	
	7.965	3.844	1.546	1.133	0.823, 0.683	
Lys17	8.595	3.897	1.827	1.316	1.598	2.787
	8.479	3.796	1.686	1.236	1.554	2.771, 2.668
Arg18	7.963	4.036	1.901, 1.667	1.417	3.150	7.281, 6.771
	7.765	3.983	1.910, 1.667	1.423	3.110	7.241
Gln19	8.113	3.998	2.023, 1.895	2.385, 2.307		7.586, 6.694
	8.368	3.843	2.004	2.262		7.300, 6.749
Asn20	8.477	4.557	2.686		7.602, 6.901	
	8.660	4.336	2.640			
Ala21	7.908	4.133	1.410			
	7.758	4.084	1.335			
Leu22	7.727	4.052	1.751, 1.640	1.528	0.781	
	7.457	4.030	1.709	1.528	0.756, 0.653	
Leu23	8.114	4.154			0.835, 0.752	
	7.979	4.023	1.738, 1.531		0.673	
Glu24	8.525	3.862	1.938	2.332, 2.135		
	8.671	3.690	1.790, 1.880	2.089		
Gln25	7.758	3.947	2.111	2.425, 2.343		7.456, 6.779
	7.604	3.871	2.137	2.437, 2.289		7.349, 6.679
Gln26	8.002	4.075	2.128, 2.054	2.443, 2.217		7.157, 6.655
	7.882	3.945	2.218, 2.033	2.491		6.984, 6.539
Val27	8.336	3.402	2.043	0.865, 0.712		
	8.378	3.265	2.032	0.821, 0.676		
Arg28	7.854	4.046	1.753	1.678, 1.609	3.111	7.343
	8.013	3.964	1.775	1.686, 1.554	3.061	7.251
Ala29	7.932	4.075	1.382			
	7.685	3.983	1.330			
Leu30	8.022	4.091			0.852, 0.776	
	7.494	4.087	1.605	1.465	0.689	
Glu31	8.306	3.997	1.907	2.128, 2.031		
	8.195	3.872	1.987, 1.831	2.343		
Lys32	7.904	4.070	1.778	1.394	1.589	2.899
	7.785	4.011	1.717	1.354, 1.270	1.514	2.801, 7.400
Ala33	7.780	4.112	1.345			
	7.596	4.044	1.301			
			(b) Myc-LZ			
Ser1		3.958	3.838, 3.788			
		4.055	3.878			
Val2	8.401	3.956	1.905	0.787		
	8.548	3.966	1.895	0.792		

Table 2 (Continued)

	chemical shifts (ppm)					
residue	HN	Hα	Hβ	Hγ	Hδ	Hε/others
Gln3	8.460	4.098	1.931, 1.855	2.235		7.426, 6.712
	8.546	4.121	1.968, 1.894	2.252		7.440, 6.755
Ala4	8.208	4.053	1.254			
	8.286	4.057	1.278			
Glu5	8.241	3.971	1.868	2.140		
	8.290	3.965	1.923	2.186		
Glu6	8.282	3.914	1.874	2.140, 2.083		
	8.112	3.821	1.944	2.151		
Gln7	8.101	3.969	1.921	2.233		7.423, 6.753
	8.087	3.901	1.937	2.240		7.374, 6.751
Lys8	7.975	4.042	1.771	1.341, 1.251	1.520	2.805
	7.880	3.978	1.609	1.249	1.525	2.812
Leu9	7.961	3.850		1.487	0.771, 0.716	
	7.569	4.096	1.715	1.564	0.670	
Ile10	8.022	3.901	1.708	1.408, 0.995, 0.765	0.670	
	7.937	3.597	1.649	1.324, 0.754	0.611	
Ser11	8.339	4.257	3.959, 3.832			
	8.192	4.182	3.929, 3.833			
Glu12	8.391	3.939	2.109, 1.944	2.248		
	8.230	3.893	1.982	2.350, 2.218		
Glu13	8.447	3.844	1.963	2.115		
	8.461	3.596	1.961	2.035		
Asp14	8.004	4.293	2.691, 2.501			
	8.007	4.212	2.696, 2.527			
Leu15	7.867	4.088	1.556	1.438	0.743, 0.681	
	7.818	3.890	1.622	1.505	0.735	
Leu16	8.013	3.903		1.447	0.760, 0.681	
	8.226	3.893	1.762	1.457	0.744	
Arg17	7.970	3.801	1.841	1.610, 1.412	3.097	7.264
	8.557	3.845	1.893, 1.797	1.657, 1.421	3.103	7.437
Lys18	7.872	3.912	1.800	1.278	1.542, 1.418	2.783
	7.817	3.930	1.846, 1731		1.649, 1.451	2.969, 2.800
Arg19	8.213	3.844	1.873, 1.804	1.644, 1.469	3.078, 2.992	
	8.116	3.964	1.796		3.102	
Arg20	7.996	3.959	1.805, 1.693	1.542, 1.452	3.020	7.184
	8.082	3.943	1.695	1.454, 1.255	2.969	7.018
Glu21	7.982	3.919	1.944	2.225, 2.115		
	7.648	3.829	1.997	2.263		
Gln22	7.855	3.981	1.959, 1.904	2.203, 2.154		7.291, 6.725
	7.892	3.970	2.095	2.545, 2.200		7.407, 6.733
Leu23	7.797	4.065	1.606	1.432	0.757, 0.709	
	7.879	3.978	1.7.15	1.356	0.830, 0.684	
Lys24	7.800	3.851	1.706	1.326, 1.165	1.474	2.786
	8.553	3.752	1.856	1.332	1.613	2.756
His25	7.835	4.347	3.077		6.979	7.942
	7.991	4.342	3.171		6.984	8.218
Lys26	7.938	3.953	1.793	1.390, 1.251	1.549	2.805
	7.997	3.969	1.721	1.239	1.533	2.801
Leu27	8.174	3.965	1.659, 1.570	1.399	0.717	
	8.248	3.779	1.582, 1.511		0.821, 0.686	
Glu28	7.954	3.993	2.077, 2.008	2.422, 2.279		
	7.696	3.803	1.997	2.239, 2.108		
Gln29	8.035	3.867	1.996, 1.933	2.249, 2.134		7.439, 6.717
	7.773	3.892	1.997	2.207, 2.074		7.276, 6.706
Leu30	7.834	4.023	1.570		0.750	
	8.123	3.962	1.539	1.367	0.685	
Arg31	7.889	4.048	1.808, 1.702	1.542, 1.452	3.022	7.132
	7.947	4.011	1.831, 1.677	1.446	2.969	7.230
Asn32	8.061	4.561	2.722, 2.620		7.488, 6.786	
	7.799	4.557	2.749, 2.622		7.509, 6.805	
Ser33	7.973	4.238	3.941, 3.824			
	7.815	4.230	3.936, 3.802			

[a] The first line for each residue gives the chemical shifts of the homomeric species and the second the value for the respective residue in the heterodimer. Peptide concentrations and buffer conditions were as in Figure 7.

DISCUSSION

In this and in a previous paper (Muhle-Goll et al., 1994), we have shown that relatively short peptides spanning the sequence of LZs from members of the HLH-LZ family can display the same dimerization behavior as the intact proteins *in vivo*. This supports the speculation that the role of the LZ in those HLH-LZ proteins that show homo- and heterodimerization is to determine the specificity of the dimerization while the stability of the dimer may be mostly determined by a HLH domain.

Intrinsic Tendency of the Peptides To Form Helices. Both the sequences of Max- and Myc-LZ have a strong tendency

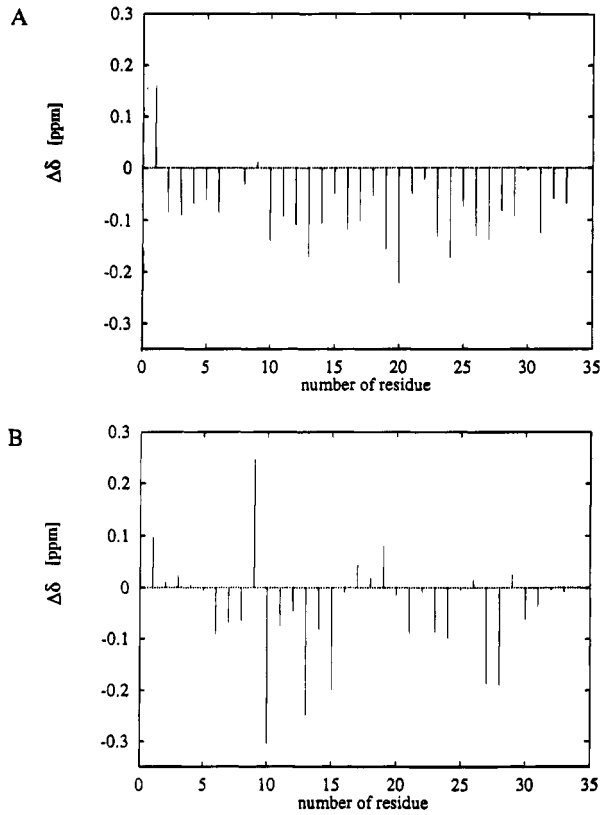

FIGURE 8: Chemical shift differences $\Delta\delta$ in ppm of the H_α frequencies of the corresponding residues in the heterodimer versus the homodimer: (A) Max-LZ and (B) Myc-LZ.

to fold as α-helices. However, the stability of the fold is highly dependent on specific solvent conditions and concentration. This has been observed in other systems (Musco et al., 1995). All the residues of the Myc and Max leucine zippers are helix stabilizers with a strong predominance of charged groups (Munoz & Serrano, 1994). However, the monomeric Myc-LZ displays a larger helicity than dimeric Max-LZ under physiological conditions. This can be explained by the larger number of intrahelical attractive polar interactions possible in Myc-LZ (see Figure 9). In addition, the sequence of the synthetic Myc-LZ contains a capping box with a serine at the helix N-terminus (Presta & Rose, 1988). The net effect of all these contributions is more clearly evident by comparison of the helicity of the two peptides in TFE, a solvent which stabilizes monomeric helices. In a 1:1 water/TFE mixture, Myc-LZ shows a higher helical content than Max-LZ.

Heterodimer Formation. The c-Myc-LZ and Max-LZ heterodimer is more stable than any of the homodimers. This is supported by several experimental results. (1) Upon mixing the two peptides, the ellipticity of the CD signal at 222 nm increases, indicating a higher amount of α-helical secondary structure. (2) The thermostability increases. (3) The dissociation constant calculated for the heterodimer at neutral pH (25 °C) is smaller (6.13×10^{-5} $M^{-1} \pm 9\%$) than for the isolated Max-LZ (20.3×10^{-5} $M^{-1} \pm 5\%$) (a value for Myc-LZ could not be calculated since dimerization could not be shown for this peptide at this pH). (4) The CD signal reaches a minimum at a 1:1 ratio of the peptides. (5) The secondary chemical shifts of the NMR Hα resonances of the Max-LZ/Myc-LZ mixture show a higher helicity for the mixture. The differential shifts of some of the resonances (Figure 8 and Table 2) indicate further that a conformational transition occurs upon heterodimer formation. Furthermore,

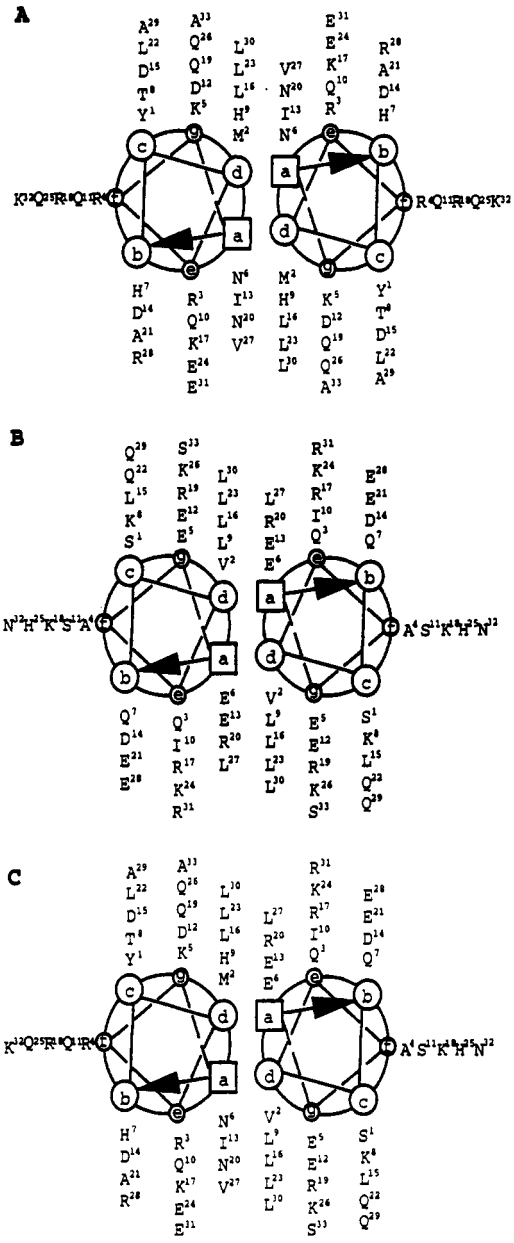

FIGURE 9: Coiled coil helical wheel representation of the sequences of the (A) Maz-LZ homodimer, (B) Myc-LZ homodimer, and (C) Max-LZ/Myc-LZ heterodimer. The residues are numbered from 1 (N-terminus) to 33 (C-terminus).

no signal of the homodimeric LZs was detectable, indicating a predominant transition to the heterodimeric species.

Tetramerization? Tetramerization has been detected for some of the HLH proteins (MyoD, Anthony-Cahill et al., 1992; myogenin, Farmer et al., 1992; MyoD/ID, Fairman et al., 1993) and HLH-LZ proteins (Myc, Dang et al., 1989; TFEB, Fisher et al., 1991). The DNA-binding domain of USF was shown to tetramerize only if the LZ part was present (Ferré-D'Amaré et al., 1994). In principle, the stabilization of the HLH-LZ leucine zippers resulting in higher helicity might also be the consequence of a three-state monomer-to-dimer-to-tetramer equilibrium. However, this hypothesis can be excluded in our case since temperature denaturation curves show a one-step transition. When the data were analyzed assuming a two-state model in which the dimer is only transiently present and the dominant species are monomer and tetramer, the K_u values calculated at different concentrations did not produce superimposable

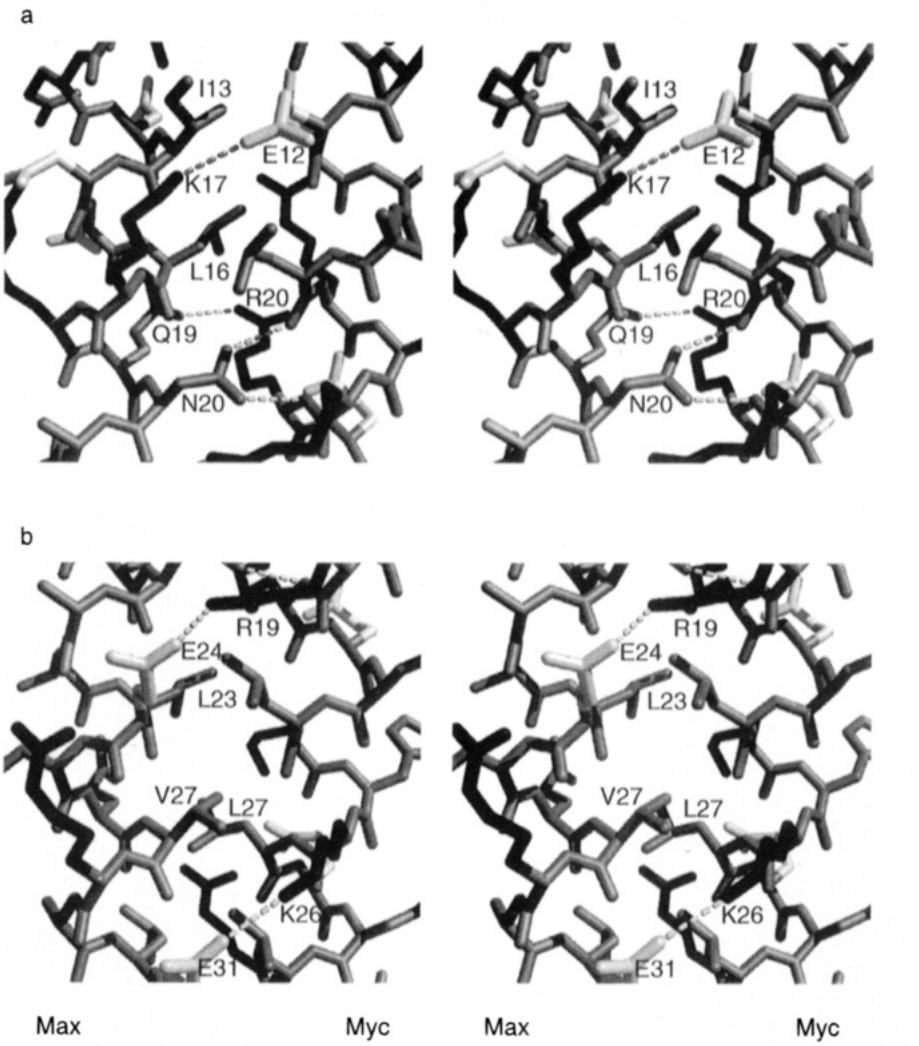

FIGURE 10: Model of the Max-LZ/Myc-LZ heterodimer. Polar interactions between the Myc-LZ and Max-LZ monomers are indicated by dashed lines. Glu and Asp side chains are light gray, Lys and Arg side chains black, and all other side chains and main chain atoms gray. (a) The region around the charged Glu13 residue in a position in Myc-LZ. (b) Two salt bridges between Myc−LZ-Arg19 and Max-LZ-Glu24 and Myc-LZ-Lys26 and Max-LZ-Glu31.

results leading to a unique dissociation constant (Figures 2 and 6).

Coiled Coil Formation. It is widely accepted that coiled coil formation can be detected by a more negative far-UV CD band at 222 nm than at 208 nm (Cooper & Woody, 1990). The spectra of both homo- and heterodimers of Max-LZ and Myc-LZ, however, behave in the opposite way, with the band at 208 nm always more negative. One possible explanation for this behavior is that the phenomenon has so far mostly been observed for very stable coiled coil systems, such as tropomyosin or model coiled coil peptides (Zhou et al., 1992; Greenfield & Hitchcock-DeGregori, 1993). The dimers described in this work have constants at least 2−3 orders of magnitude lower. We therefore expect that, even at room temperature, the equilibrium between a helical dimer and the unfolded monomer is significantly shifted toward the latter. The intensity of the minimum at 208 nm undoubtedly contains both contributions and could easily be distorted.

Factors Stabilizing the Homo- and Heterodimers. The stability of the heterodimer is determined by interactions between residues in the interface in much the same way as, for example, in coiled coils of the b-Zip family. There are, however, some differences in the residues that form the interface of the putative homodimers of Max-LZ or Myc-LZ (Figure 9); Max-LZ has a His and a Met residue on the first two d positions usually occupied by Leu. In GCN4, replacement of more than one Leu by any other amino acid was shown to reduce the stability of the dimer (Hu et al., 1990b). Several residues on the a positions contribute as well to a weakening of the hydrophobic interaction; Max-LZ has two Asn residues on this position, while members of the b-Zip family, like GCN4 and Jun, have only one. Myc-LZ has two Glu and one Arg on a positions. In comparison, Fos, the most polar partner in the Jun-Fos system, has two Lys residues on a positions. Lys is generally tolerated at this position in coiled coils (Cohen & Parry, 1990), since it can contribute to the hydrophobic interaction. Both Glu residues in a positions in Myc-LZ are flanked by Glu residues on g positions. This alone is presumably a very efficient mechanism for destabilizing the homodimer of Myc-LZ under physiological conditions, since the Glu side chains on a positions would be untolerably close to those on the g′ position (cf. also Figure 10A, which shows a model of the heterodimer). As already discussed in our previous paper (Muhle-Goll et al., 1994), the homodimer of Myc-LZ is also disfavored because of repulsive electrostatic interactions between e and g positions.

None of these repulsive electrostatic interactions is present in the heterodimer. An Ile side chain at the a position in

Max-LZ can pack between the two Glu side chains at the g and a positions in Myc-LZ (Figure 10A). The e/g′ interactions match perfectly in the Myc-LZ/Max-LZ heterodimer; four out of eight corresponding e and g positions are occupied by oppositely charged residues. In the remaining positions, two positively charged Arg and Lys and a negatively charged Glu in the g position in Myc-LZ are opposite to a Gln at the corresponding e position in Max. Most of the putative e/g′ interactions between the monomers form in the model (Figure 10B). An exception is the salt bridge between Myc-LZ-Arg17 and Max-LZ-Asp12. However, the Asp side chain may be too short to form a salt bridge, as also suggested by the low occurrence of Asp in the e and g positions of b-Zip LZs (Vinson et al., 1993). The charged residues in position a in Myc-LZ can make polar interactions with the g positions in Max-LZ. Myc-LZ Glu6 can form a salt bridge with Max-LZ Lys5, while Myc-LZ Arg20 can make a polar interaction with Max-LZ Glu19. Thus, the a positions added to the stability of the heterodimer by additional polar contacts.

Overall, the lower stability even of the heterodimer as compared to that of any member of the b-Zip protein family is consistent with the presumed role of the LZ in the HLH-LZ domain, that is, to confer dimerization specificity. This is also indicated by *in vivo* experiments performed to date (Amati et al., 1993).

ACKNOWLEDGMENT

We are grateful to R. Jacob for extensive HPLC analysis to check the purity of the samples.

REFERENCES

Amati, B., Brooks, M. W., Levy, N., Littlewood, T. D., Evan, G. I., & Land, H. (1993) *Cell 72*, 233−245.
Anthony-Cahill, S. J., Benfield, P. A., Fairman, R., Wasserman, Z. R., Brenner, S. L., Stafford, W. F., III, Altenbach, C., Hubbel, W. L., & DeGrado, W. F. (1992) *Science 255*, 979−983.
Ayer, D. E., & Eisenman, R. N. (1993) *Genes Dev. 7*, 2110−2119.
Ayer, D. E., & Kretzner, L., & Eisenman, R. N. (1993) *Cell 72*, 211−222.
Bairoch, A., & Boeckmann, B. (1991) *Nucleic Acids Res. 19*, 2247−2249.
Baxevanis, A. D., & Vinson, C. R. (1993) *Curr. Opin. Genet. Dev. 3*, 278−285.
Beckmann, H., & Kadesch, T. (1991) *Genes Dev. 5*, 1057−1066.
Blackwood, E., & Eisenman, R. N. (1991) *Science 251*, 1211−1217.
Bohmann, D., Bos, T. J., Admon, A., Nishimura, T., Vogt, P. K., & Tijan, R. (1987) *Science 238*, 1386−1392.
Brünger, A. T. (1992) *X-PLOR. A System for X-ray Crystallography and NMR*, Yale University Press, New Haven, CT.
Cao, Z., Umek, R. M., & McKnight, S. L. (1991) *Genes Dev. 5*, 1538−1552.
Chen, Y.-H., Yang, J. T., & Chau, K. H. (1974) *Biochemistry 13*, 3350−3359.
Cohen, C., & Parry, D. A. D. (1990) *Proteins 7*, 1−15.
Cooper, T. M., & Woody, R. W. (1990) *Biopolymers 30*, 657−676.
Dang, C. V., McGuire, M., Buckmire, M., & Lee, W. M. F. (1989) *Nature 337*, 664−666.
Davis, L. J., & Halazonetis, T. D. (1993) *Oncogene 8*, 125−132.
Davis, R. L., Cheng, P.-F., Lassar, A. B., & Weintraub, H. (1990) *Cell 60*, 733−746.
Evan, G. I., & Littlewood, T. D. (1993) *Curr. Opin. Genet. Dev. 3*, 44−49.
Fairman, R., Beran-Steed, R. K., Anthony-Cahill, S. J., Lear, J. D., Stafford, W. F., III, DeGrado, W. F., Benfield, P. A., & Brenner, S. L. (1993) *Proc. Natl. Acad. Sci. U.S.A. 90*, 10429−10433.
Farmer, K., Catala, F., & Wright, W. E. (1992) *J. Biol. Chem. 267*, 5631−5636.
Ferré-D'Amaré, A. R., Prendergast, G. C., Ziff, E. B., & Burley, S. K. (1993) *Nature 363*, 38−45.
Ferré-D'Amaré, A. R., Pognonec, P., Roeder, R. G., & Burley, S. K. (1994) *EMBO J. 13*, 180−189.
Fisher, D. E., Carr, C. S., Parent, L. A., & Sharp, P. A. (1991) *Genes Dev. 5*, 2342−2352.
Frank, R., & Gausepohl, H. (1988) in *Modern Methods in Protein Chemistry* (Tschesche, H., Ed.) Vol. 3, pp 41−60, de Gruyter, Berlin.
Greenfield, N. J., & Hitchcock-DeGregori, S. E. (1993) *Protein Sci. 2*, 1263−1273.
Gregor, P. D., Sawadogo, M., & Roeder, R. G. (1990) *Genes Dev. 4*, 1730−1740.
Griesinger, C., Otting, G., Wüthrich, K., & Ernst, R. R. (1988) *J. Am. Chem. Soc. 110*, 7870−7872.
Hai, T., Liu, F., Coukos, W. J., & Green, M. R. (1989) *Genes Dev. 3*, 2083−2090.
Hu, J. C., O'Shea, E. K., Kim, P. S., & Sauer, R. T. (1990b) *Science 250*, 1400−1403.
Hu, Y.-F., Lüscher, B., Admon, A., Mermod, N., & Tjian, R. (1990a) *Genes Dev. 4*, 1741−1752.
Jeener, J., Meier, B. H., Bachmann, P., & Ernst, R. R. (1979) *J. Chem. Phys. 71*, 4546−4553.
Kadkhodaei, M., Hwang, T.-L., Tang, J., & Shaka, A. J. (1993) *J. Magn. Reson. 105*, 104−107.
Kato, G. J., Lee, W. M. F., Chen, L., & Dang, C. V. (1992) *Genes Dev. 6*, 81−92.
Krylov, D., Mikhailenko, I., & Vinson, C. (1994) *EMBO J. 13*, 2849−2861.
Larsson, L.-G., Petterson, M., Öberg, F., Nilsson, K., & Lüscher, B. (1994) *Oncogene 9*, 1247−1252.
Macura, S., Huang, Y., Suter, D., & Ernst, R. R. (1981) *J. Magn. Reson. 43*, 259−281.
Marion, D., & Wüthrich, K. (1983) *Biochem. Biophys. Res. Commun. 113*, 967−974.
Muhle-Goll, C., Gibson, T., Schuck, P., Schubert, D., Nalis, D., Nilges, M., & Pastore, A. (1994) *Biochemistry 33*, 11296−11306.
Munoz, V., & Serrano, L. (1994) *Nat. Struct. Biol. 1*, 399−409.
Musco, G., Tziatzios, C., Schuck, P., & Pastore, A. (1995) *Biochemistry 34*, 553−561.
Nilges, M. (1995) *J. Mol. Biol. 245*, 645−660.
Nilges, M., & Brünger, A. T. (1991) *Protein Eng. 4*, 649−659.
O'Shea, E. K., Klemm, J. D., Kim, P. S., & Alber, T. (1991) *Science 254*, 539−544.
O'Shea, E. K., Rukowski, R., & Kim, P. S. (1992) *Cell 68*, 699−708.
Pastore, A., & Saudek, V. (1990) *J. Magn. Reson. 74*, 557−564.
Presta, L. G., & Rose, G. D. (1988) *Science 240*, 1632−1641.
Thompson, K. S., Vinson, C., & Freire, E. (1993) *Biochemistry 32*, 5491−5496.
Vinson, C. R., Hai, T., & Boyd, S. M. (1993) *Genes Dev. 7*, 1047−1058.
Voronova, A., & Baltimore, D. (1990) *Proc. Natl. Acad. Sci. U.S.A. 87*, 4722−4726.
Weiss, M. A. (1990) *Biochemistry 29*, 8020−8024.
Williams, S. C., Cantwell, C. A., & Johnson, P. (1991) *Genes Dev. 5*, 1553−1567.
Wishart, D. S., Sykes, B. D., & Richards, F. M. (1991) *J. Mol. Biol. 222*, 311−333.
Wüthrich, K. (1986) *NMR of Proteins and Nucleic Acids*, John Wiley & Sons, New York.
Zervos, A. S., Gyuris, J., & Brent, R. (1993) *Cell 72*, 223−232.
Zhou, N. E., Kay, C. M., & Hodges, R. S. (1992) *J. Biol. Chem. 267*, 2664−2670.
Zhou, N. E., Kay, C. M., & Hodges, R. S. (1994) *J. Mol. Biol. 237*, 500−512.

BI950277P